

EXPERIMENTAL STUDY ON ROTATIONAL BEHAVIOR OF CLT SHEAR WALL-I STEEL LINK BEAM CONNECTIONS

Mingqian Wang¹, Yubing Leng², Xi Chen³, Qingfeng Xu^{4*}

ABSTRACT: This paper presents the experimental results of rotational behavior of CLT shear wall-I steel link beam connections. Three full-scale connection specimens were prepared and tested under monotonic and reversed cyclic loading. Test results indicated that the typical failure modes of the specimens were tensile fracture failure of the flange at the bottom of the I-beam and shear failure of the web. No obvious damage occurred in the CLT shear wall. This demonstrated that the steel link beams can effectively reduce seismic damage to the CLT shear walls and serve as the first line of seismic defense. At the initial stage of loading, the bending moment-rotation angle curve of each specimen showed a linear stage. Different from the rotational performance of the bolted glulam beam-to-column connections, there was no obvious low-stiffness slip section in the specimens during the initial loading period. When the load level was over 60% of the peak load, the specimen entered the nonlinear stage. When the tensile fracture failure of the flange occurred, the moment bearing capacity of the specimens reduced significantly. The bending capacity of the monotonically loaded specimen was 8.8% higher than the average values of the reversed cyclic loading specimens. The ductility ratio of each specimen was close to 3.0, indicating that the steel link beam connection exhibited excellent ductility.

KEYWORDS: cross laminated timber, I steel link beam, connection, rotational behavior

1 – INTRODUCTION

Cross laminated timber (CLT) is an engineered wood product made by gluing layers of dimension lumber in an alternating orthogonal pattern to fabricate large scale solid panels [1]. CLT panels are widely used as shear walls and floor diaphragms in multi-story and high-rise timber structures [2-3]. However, the bottom CLT shear walls of the timber structures can be easily damaged under earthquake excitations. Therefore, it is important to improve the seismic performance of the CLT shear walls and change the typical failure modes of the CLT shear walls. A combination of the CLT panels and I steel link beams is a good way to improve the seismic performance of the CLT shear walls. Rotational behavior of the connections between the steel beam and CLT shear wall is critical for design of the structures. This paper presents the experimental results of rotational behavior of CLT shear wall-I steel link beam connections. Three full-

scale connection specimens were prepared and tested under monotonic and reversed cyclic loading tests. The research can provide guide for design and application of CLT shear wall-I steel link beam structures.

2. EXPERIMENTAL PROGRAM

2.1 SPECIMEN DETAILS & MATERIALS

Three full-scale CLT shear wall-I steel link beam connection specimens were designed and prepared for testing. One specimen was subjected to monotonic loading, and the other two specimens were subjected to reversed cyclic loading.

Detailed specimen geometry is shown in Figure 1. The specimen included one CLT shear wall and one I steel link beam. The CLT shear wall had five layers of dimension lumber with each layer thickness of 35 mm. The height and cross section length of the CLT shear wall

¹ Mingqian Wang, Shanghai Research Institute of Building Sciences Co. Ltd, Shanghai, China, glulam_wmq@163.com

² Yubing Leng, Shanghai Research Institute of Building Sciences Co. Ltd, Shanghai, China, leng_yb@163.com

³ Xi Chen, Shanghai Research Institute of Building Sciences Co. Ltd, Shanghai, China, cx541026@hotmail.com

⁴ Qingfeng Xu, corresponding author, Shanghai Research Institute of Building Sciences Co. Ltd, Shanghai, China, xqingfeng73@163.com

were 2000 mm and 800 mm, respectively. The I steel link beam had a total length of 600 mm. The section height, width, web thickness and flange thickness were 140 mm, 80 mm, 5.5 mm and 9.1 mm respectively. The steel link beam were connected to the CLT shear wall by using steel plates perpendicular to the I-beam section, slotted-in steel plates and bolts. The steel plates were connected by welding, and the leg size of the fillet weld was 10 mm. The cross-sectional dimensions of the steel plate perpendicular to the I-beam section and the slotted-in steel plate were 175 mm × 700 mm and 300 mm × 700 mm, respectively. To facilitate processing, the thickness of both steel plates was 10 mm. The slot size of the shear wall was 12 mm. To avoid premature failure of the slotted-in steel plate bolt connection, the number of bolts in bolt joints was increased to 20. This design can ensure that the bolt joints would not be damaged, and at the same time reduce the influence of factors such as the initial clearance of the bolts, and maximize the initial stiffness of the connection. Bolt diameter and spacing were 12 mm and 100 mm respectively.

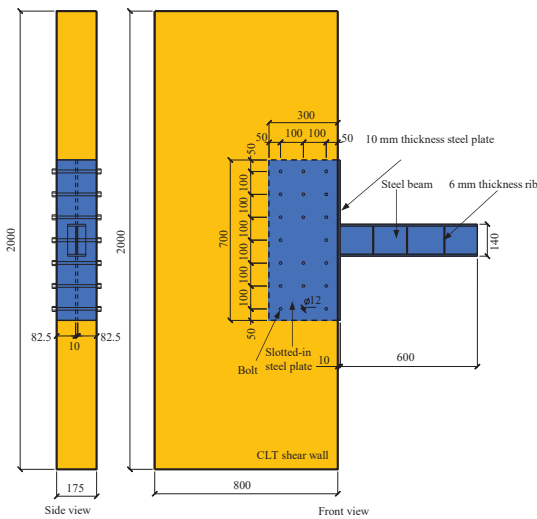


Figure 1. Detailed specimen geometry (Unit: mm)

The CLT shear walls were made of S-P-F. Material mechanical property parameters of S-P-F were determined through small clear specimen tests, as shown in Table 1. The measured density and moisture content of spruce-pine-fir are 425 kg/m³ and 13.1%, respectively. The steel plate was made of Q235 steel, and the measured yield strength was 300 MPa. The bolts were grade 8.8 ordinary bolts with a yield strength of 640 MPa.

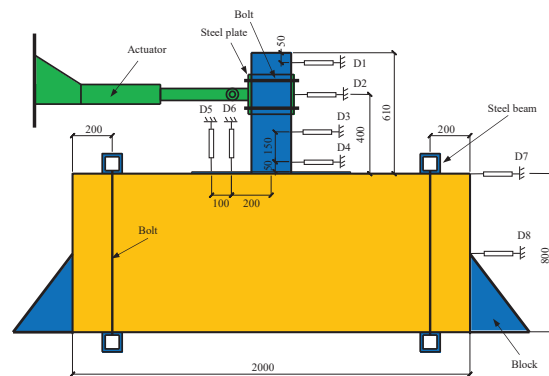
Table 1: Material mechanical properties of S-P-F

Mechanical properties	Averaged values
Longitudinal tensile elastic modulus	10980 MPa
Longitudinal tensile strength	64.8 MPa

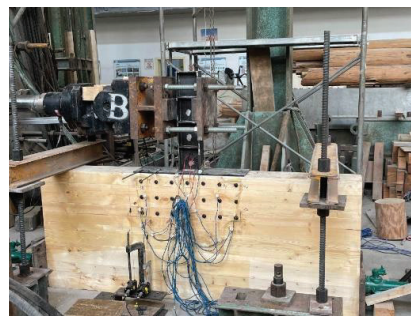
Longitudinal compressive elastic modulus	15690 MPa
Longitudinal compressive strength	32.8 MPa
Bending elastic modulus	12750 MPa
Bending strength	66.6 MPa
Longitudinal shear strength	7.8 MPa

2.2 TEST PROTOCOL

Test setup and data measurement scheme is shown in Figure 2. The specimen was initially rotated 90° and placed on the test platform, and the CLT shear wall was fixed through steel beams, bolts and steel blocks. Then the free end of the link beam was loaded by using a horizontally placed actuator. Considering that the clear span of connecting beams in the CLT shear wall was relatively limited, the vertical distance from the center of the loading point to the top surface of the CLT wall was 400 mm. The loading rate was controlled at 5 mm/min.



(a) Test setup and data measurement scheme



(b) Testing view

Figure 2. Test setup and data measurement scheme (Unit: mm)

The test steps for monotonic loading are as follows: the specimen was pre-loaded up to 10% of the estimated ultimate load and maintained for 2 mins to check the working status of the measuring device used in the test and to eliminate bad contact between the bolt and other components. After unloading, the specimen were

continuously loaded up to failure or the load was reduced to 80% of the peak load.

Reversed cyclic horizontal loads were applied under displacement control mode according to the commonly used test method for timber structures ASTM E 2126 (Test method B) [4]. The specimens were also pre-loaded up to 10% of the estimated ultimate load and maintained for 2 mins. The reversed cyclic loading scheme started with five single fully-reversed cycles having horizontal displacement amplitude of 1.25Δ , 2.5Δ , 5.0Δ , 7.5Δ and 10Δ . Following this, three fully-reversed cycles were performed from horizontal displacement amplitude of 20Δ with increments of 20Δ until failure. Δ was the reference displacement determined based on monotonic loading test.

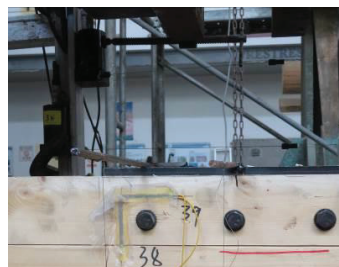
Test measurement items included horizontal loads and link beam angles. Among them, the horizontal load was measured by the force sensor built into the actuator. The rotation angle of the link beam was calculated from the horizontal displacement distribution of the coupling beam along its height direction during the loading process measured by the displacement meter. The layout of the LVDTs is shown in Figure 2a. D1 and D2 were used to measure the horizontal displacement of the top of the link beam and the actuator; D3 and D4 were used to measure the rotation angle of the link beam; D5 and D6 were used to measure the rotation angle of the steel plate perpendicular to the I-beam section; D7 and D8 were used to monitor the horizontal displacement of the CLT shear wall.

3 – TEST RESULTS & DISCUSSION

3.1 TYPICAL FAILURE MODES

Typical failure modes of all specimens are similar, therefore specimen S2 was used to illustrate the failure process of the connections, as shown in Figure 3. As the horizontal displacement reached 6 mm, one side of the steel plate perpendicular to the I-beam section compressed with the top surface of the CLT shear wall (Figure 3a), and there was a separation between the steel plate and the CLT shear wall (Figure 3b). When the horizontal displacement was up to 18 mm, there was a gap between the steel plate perpendicular to the I-beam section and the CLT shear wall at the middle part of the connection (Figure 3c). When the horizontal displacement was up to 24 mm, tensile fracture failure occurred in the weld between the I-beam and the steel plate perpendicular to the I-beam section due to the large bending moment (Figure 3d). As the displacement increasing, the tensile cracks propagated through the I-beam cross section. Finally, the total cross section of the

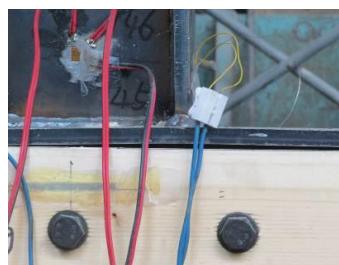
I-beam fractured (Figure 3f). No obvious damage occurred in the CLT shear wall. This implied that the steel link beams can effectively reduce seismic damage to the CLT shear walls and serve as the first line of seismic defense.



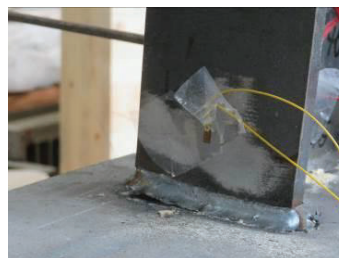
(a) Compression between steel plate and CLT



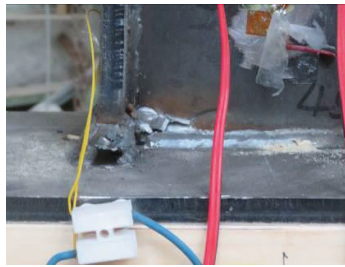
(b) Separation between steel plate and CLT



(c) Gap between steel plate and CLT



(d) Tensile failure of the weld



(e) Crack propagation

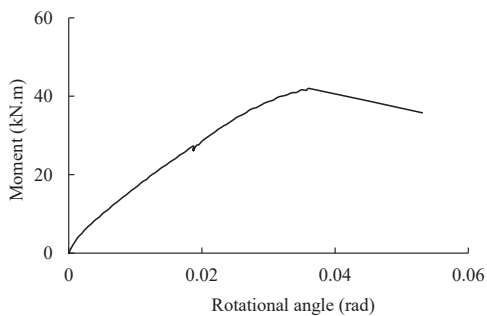


(f) Tensile fracture failure

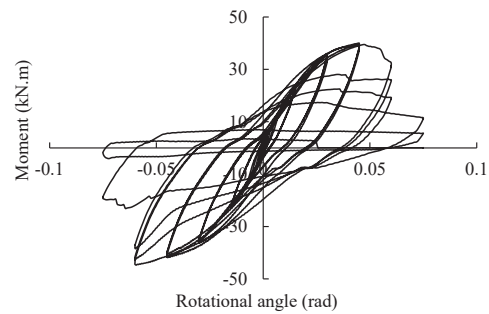
Figure 3. Typical failure modes of specimen S2

3.2 MOMENT-ROTATIONAL ANGLE CURVES

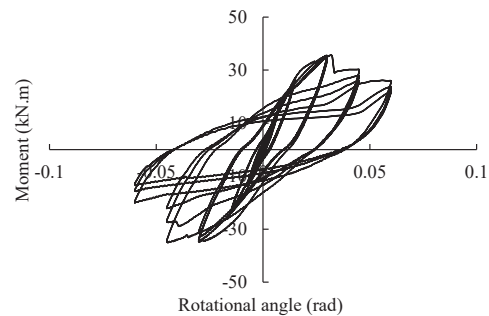
Moment-rotational angle curves of all specimens are shown in Figure 4. At the initial stage of loading, the bending moment-rotation angle curve of each specimen showed a linear stage. Different from the rotational performance of the bolted glulam beam-to-column connections, there was no obvious low-stiffness slip section in the specimens during the initial loading period. When the load level was over 60% of the peak load, the specimen entered the nonlinear stage. When the tensile fracture failure of the flange occurred, the moment bearing capacity of the specimens reduced significantly.



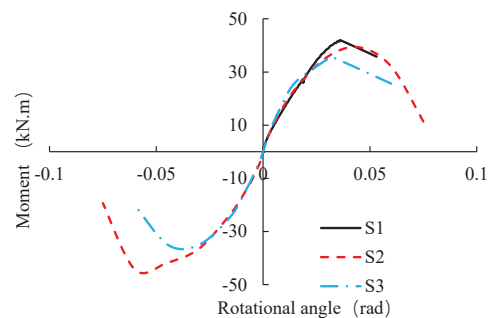
(a) Specimen S1



(b) Specimen S2



(c) Specimen S3



(d) Skeleton curves

Figure 4. Moment-rotational angle curves of all specimens

3.3 KEY MECHANICAL PARAMETERS

Key mechanical parameters of all specimens are listed in Table 2. More specifically, maximum bending moment M_{max} and its corresponding rotational angle θ_{max} were determined by the peak points of the skeleton curves. Ultimate failure bending moment M_u and its corresponding rotational angle θ_u were determined by 85% of the maximum bending moment after peak points and its corresponding rotational angle. Initial stiffness k was determined by the ratio of 40% of the maximum bending moment to its corresponding rotational angle. Yielding bending moment and its corresponding rotational angle was determined by equivalent Energy Elastic-Plastic

(EEEP) method [5]. Ductility ratio was the ratio of rotational angle of failure bending moment to rotational angle of yielding bending moment.

Table 2: Key mechanical parameters of all specimens

Specimen ID	k	M_y	θ_y	M_{max}	θ_{max}	M_u	θ_u	μ
	/kN.m/rad	/kN.m	/rad	/kN.m	/rad	/kN.m	/rad	
S1	1665	35.3	0.021	42.0	0.036	35.7	0.053	2.5
S2+	1789	32.6	0.018	39.3	0.045	33.4	0.057	3.1
S2-	1668	36.2	0.022	44.3	0.060	37.7	0.064	2.9
S3+	2036	32.0	0.015	35.7	0.032	30.4	0.047	3.1
S3-	1798	31.8	0.018	35.1	0.044	29.8	0.050	2.8

As seen from Table 2, the bending moment capacity of the monotonically loaded specimen was 8.8% higher than the average value of the reversed cyclic loading specimens, which was mainly due to the more significant cumulative damage of the specimens under reversed cyclic loading. The bending moment capacity of specimen S2 was 18.1% higher than that of specimen S3. The displacement amplitudes corresponding to the tension side flange welds of specimens S2 and S3 being pulled apart were 24 mm and 18 mm, respectively. This indicated that the difference in welding quality had an important impact on the bending moment capacity of the steel link beams. The ductility ratio of each specimen was close to 3.0, indicating that the excellent ductility of the steel link beam connection specimen.

4 – CONCLUSION

1) The typical failure modes of the specimens were tensile fracture failure of the flange at the bottom of the I-beam and shear failure of the web. No obvious damage occurred in the CLT shear wall. This demonstrated that the steel link beams can effectively reduce seismic damage to the CLT shear walls and serve as the first line of seismic defense.

2) At the initial stage of loading, the bending moment-rotation angle curve of each specimen showed a linear stage. Different from the rotational performance of the bolted glulam beam-to-column connections, there was no obvious low-stiffness slip section in the specimens during the initial loading period. When the load level was over 60% of the peak load, the specimen entered the nonlinear stage. When the tensile fracture failure of the flange occurred, the moment bearing capacity of the specimens reduced significantly.

3) The bending moment capacity of the monotonically loaded specimen was 8.8% higher than the average value of the reversed cyclic loading specimens due to the more

significant cumulative damage of the specimens under reversed cyclic loading. The bending moment capacity of specimen S2 was 18.1% higher than that of specimen S3 due to the difference in welding quality of the two specimens.

4) The ductility ratio of each specimen was close to 3.0, indicating that the excellent ductility of the steel link beam connection specimen.

5 – ACKNOWLEDGEMENTS

This research was supported financially by National Natural Science Foundation of China (No. 52378522) and Research and Development Project of Ministry of Housing and Urban-Rural Development of People's Republic of China (No. 2022-K-051). The authors gratefully acknowledge the support.

6 – REFERENCES

- [1] Z. Li, X. Wang, M. He. (2022) Experimental and analytical investigations into lateral performance of cross laminated timber (CLT) shear walls with different construction methods. *Journal of Earthquake Engineering*, 26(7): 3724-3746.
- [2] Y. Jiang, R. Crocetti. (2019) CLT-concrete composite floors with notched shear connectors. *Construction and Building Materials*, 195: 127-139.
- [3] J. Cao, H. Xiong, Z. Wang, et al. (2020) Experimental investigation and numerical analysis for concrete-CLT connections. *Construction and Building Materials*, 236: 117533.
- [4] Standard test methods for cyclic (reversed) load test for shear resistance of vertical elements of the lateral force resisting systems for buildings: ASTM E2126-11 [S]. Pennsylvania, United States: ASTM, 2018.

[5] A. Jorissen, M. Fragiaco. General notes on ductility in timber structures [J]. *Engineering Structures*, 2011, 33(11): 2987-2997.